# Preparation, Characterization, and Photophysical Study of Thiazine Dyes within the Nanotubes and Nanocavities of Silicate Host: Influence of Titanium Dioxide Nanoparticle on the Pr...

**ARTICLE** *in* THE JOURNAL OF PHYSICAL CHEMISTRY C · MARCH 2010

Impact Factor: 4.77



**4 AUTHORS**, INCLUDING:

Karuppannan Senthilkumar
National University of Singapore
**14** PUBLICATIONS **58** CITATIONS
SEE PROFILE

Parimal Paul
Central Salt and Marine Chemicals Researc...
**117** PUBLICATIONS **1,838** CITATIONS
SEE PROFILE

Selvaraju Chellappan
University of Madras
**8** PUBLICATIONS **97** CITATIONS
SEE PROFILE

# Preparation, Characterization, and Photophysical Study of Thiazine Dyes within the Nanotubes and Nanocavities of Silicate Host: Influence of Titanium Dioxide Nanoparticle on the Protonation and Aggregation of Dyes

**Karuppannan Senthilkumar,[†] Parimal Paul,[‡] Chellappan Selvaraju,[†] and Paramasivam Natarajan*,[†]**

*National Centre for Ultrafast Processes, Taramani Campus, University of Madras, Chennai-600 113, India, and Central Salt and Marine Chemical Research Institute, Bhavnagar-364 002, India*

*Received: December 31, 2009; Revised Manuscript Received: March 18, 2010*

The photophysical properties of thionine and methylene blue have been investigated in the absence and presence of titanium dioxide nanoparticles encapsulated into the different nanoporous silicate materials: zeolite-Y, ZSM-5, and MCM-41. The titanium dioxide loaded zeolite samples were prepared by the ion-exchange method and the formation of $TiO_2$ nanoparticles into the zeolite host materials was ascertained by UV−visible diffuse reflectance spectroscopy and ICP-OES measurement. The crystallinity of the silicate host was found to be intact as characterized by powder X-ray diffraction, nitrogen adsorption and desorption isotherm studies and TEM. The encapsulation of $TiO_2$ into the zeolite host leads to the protonation of the dyes, indicating that the acidity of channels increased significantly in the presence of titanium dioxide in the zeolite host. In the case of zeolite-Y, with increasing loading of titanium dioxide nanoparticles, the aggregation of dyes is found to decrease. The absorption and emission spectra of the dyes, thionine and methylene blue, encapsulated into the nanochannel of ZSM-5 show a shift as compared to the spectra of the dyes in aqueous solution indicating that the planarity of the dye was perturbed due to the confinement effect of the nanochannels. ZSM-5 host with encapsulated titanium dioxide nanoparticles shows an increase in the fluorescence intensity of thionine present in the channels that is attributed to the presence of the dye in hydrophobic channels of the ZSM-5 host. The influence of the hydrophobic environment of the host on dye in the excited state was investigated by the pico- and femtosecond time-resolved spectral studies. The *N*-methyl-substituted analogue of thionine, methylene blue shows a different behavior due to the bulky nature of the dye. The aggregation of methylene blue in the cavities of zeolite-Y is less prevalent and the isomeric forms of the dye are not observed in this case in the excited state of the dye in the host channel.

## 1. Introduction

Photochemical activation of organic dyes in controlled molecular environments is an important area of research for application in photodevices and renewable energy sources.[1,2] Different microheterogeneous environments such as micelles, thin films, and silicate materials[3−6] are employed as models for photochemical processes occurring in photosynthesis and in solar energy conversion devices.[7−9] Zeolites are attractive materials for encapsulating the visible light absorbing dyes, metal complexes, and semiconductor nanoparticles which provide a steric and electrostatic environment for the guest species.[10,11] The nanochannels and cavities of the host provide additional avenues for enhancing the fluorescence lifetime including the lifetimes of the triplet state and free radicals which facilitate energy transfer and charge transfer processes.[12] Developing novel photocatalysts and understanding the relationship between local zeolite structure in the presence of $TiO_2$ nanoparticles and catalytic activity remain an important goal in heterogeneous catalysis and reaction engineering.

The aggregation of the dye molecules on a semiconductor surface has been generally viewed as detrimental to the performance of light energy conversion divices.[13,14] The dye aggregates have distinct absorption in the visible region compared to the monomers in many cases: design of systems wherein controlled energy transfer from the excited state of aggregates to monomer could be achieved to increase the efficiency of energy conversion pathway. The role of molecular aggregates as photosensitizers in color photography has been well recognized.[15−17] Spectroscopic studies on the role of the excited state of dye aggregates in these processes are rather limited. An earlier report[18] demonstrates that such aggregates can transfer triplet energy to the monomer form of the dye, which can serve as an active participant in the energy conversion process. Thus controlling the ratio of different aggregates and monomer form of the dyes can be used as energy harvesting antenna materials in the wider band of the solar spectrum.

The aggregation properties of dyes within zeolites are controlled by various factors; the aggregation properties of thionine molecules within zeolites host has been reported earlier,[19] with phenanthrene as a coguest molecule. In the presence of phenanthrene, thionine also forms aggregation with the coguest molecule. In the present investigation, semiconductor nanoparticles of $TiO_2$ are used as guest species along with the organic dyes within the zeolite host, which suppresses aggregate formation thus increasing the efficiency of the systems for the energy transfer process. Semiconductor $TiO_2$ particles have been investigated extensively for environmental photocatalyst, photoelectroclinical, solar energy conversion, and photodecompo-

* To whom correspondence should be addressed. E-mail: pnatrajan@hotmail.com.
[†] University of Madras.
[‡] Central Salt and Marine Chemical Research Institute.

10.1021/jp912267q 
Published on Web 03/30/2010

sition of $H_2O$ into $H_2$ and $O_2$ application.[20−22] Semiconductor $TiO_2$ nanoparticles are one of the most widely used photocatalyst systems because of the inertness of the semiconductor biologically and chemically and they are also photostable on absorption in the near-ultraviolet region. A large volume of research on $TiO_2$ deals with photocatalytic activities of $TiO_2$ with zeolite used as the solid support for the semiconductor.[23,24] The thiazine dyes, such as thionine ($Th^+$) and methylene blue ($MB^+$), have been studied for their photodamaging effect on DNA[25,26] and it was suggested that the binding mode of the photosensitizer could influence the photoreaction mechanism. These dyes form an important group of organic compounds that have a variety of industrial and therapeutic applications. Thionine and methylene blue have been used as an indicator dye to probe the local proton environment within the nafion film.[27]

In the present investigation, formations of $TiO_2$ within the micro- and mesoporous host materials were characterized by XRD, surface area measurement, and diffuse reflectance spectroscopy. Influence of $TiO_2$ nanoparticles on the protonation and aggregation of thionine and methylene blue within nanochannels and nanocavity of zeolites host was investigated using steady state, picosecond and femtosecond time-resolved fluorescence spectral methods.

## 2. Experimental Section

**2.1. Materials.** Zeolite-Y and ZSM-5 purchased from Sud Chemi India are washed with 1 M NaCl for about 2 h and calcined at 530 °C for 12 h. Thionine ($Th^+$) and methylene blue ($MB^+$) obtained from Aldrich Chemicals were used after recrystallizing in ethanol. Cetyltrimethylammonium bromide (CTAB), tetramethylorthosilicate (TEOS), and ammonium titanium oxalate were purchased from Lancaster. All other chemicals obtained from Qualigens were analytical grade and were used as supplied.

**2.2. Sample Preparation.** MCM-41 was synthesized and characterized by the procedure already reported in the literature.[28] A 2.4 g sample of CTAB was dissolved in 120 mL of deionized water and the mixture was stirred until the solution was homogeneous and clear. Ammonium hydroxide (8 mL) was added to this mixture with stirring for 5 min after which tetraethylorthosilicate (10 mL) was added to give a molar composition of the gel (1 M TEOS:1.64 M $NH_4OH$:0.15 M CTAB:126 M $H_2O$). The reaction mixture was stirred overnight, after which the solution was filtered and washed consecutively with deionized water and ethanol; calcination was performed at 823 K for 5 h. The obtained material was characterized by SAXRD and surface area analysis and found to show identical characteristics as reported earlier.[24]

Titanium-exchanged zeolites were prepared via an ion exchange method[29] with a ($5 \times 10^{-3}$ M) stock solution of aqueous potassium titanium oxalate. In this method 1.0 g of zeolite was stirred with ($5 \times 10^{-3}$ M) stock solution of titanium oxalate for 24 h, when formation of $TiO^{2+}$ zeolites occurs. Stirring of potassium titanium oxalate with zeolite in aqueous solution for 24 h results in the ion exchange of $Na^+$ by $TiO^{2+}$. The titanium-exchanged zeolite sample was washed with an excess of distilled water and then dried in a vacuum desiccator. As a standard procedure[30] formation of titanium dioxide nanoparticles into the channels or cavities of zeolites was achieved by heating the sample at 150 °C for 6 h. Increasing the loading of titanium dioxide within the channels or cavities was achieved by successive ion exchange followed by heat treatment. The actual amount of titanium present in the zeolite host was determined by the ICP-OES method. Calculated quantities of titanium-loaded zeolites were dissolved in 4% HF solution and a sample quantity of this solution was diluted with distilled water. The pH of the solution was adjusted to the neutral solution with use of barium sulfate as a base and titanium was estimated.

The aqueous solution of the dyes $Th^+$ and $MB^+$ and zeolites was stirred for 4 h at room temperature and washed with an excess of distilled water, which results in the dyes being exchanged with the cations present in the zeolite samples. As the molecular size of the dyes is smaller than that of the zeolite pore opening, the dye becomes encapsulated into the channels or cavities of zeolites. The concentration of the dyes in zeolites was varied from $1 \times 10^{-6}$ (mol of dye)/(g of zeolite) to $1 \times 10^{-3}$ (mol of dye)/(g of zeolite). A similar procedure was followed for $Th^+$ and $MB^+$ encapsulated into the $TiO_2$ loaded zeolites, MCM-41 and silica. The silicate samples encapsulated with the dyes are washed thoroughly to remove the dyes adsorbed onto the external surface of the host.

**2.3. Characterization.** BET surface area, pore volume, and pore size distribution of $TiO_2$ loaded zeolite samples were performed with use of volumetric adsorption equipment (ASAP 2010 micrometric USA) at 77 K. The sample was degassed under vacuum at 373 K prior to data collection. Powder X-ray diffraction patterns were recorded using a diffractometer with Cu Kα radiation ($\lambda = 1.5406$ Å). Transmission electron microscopy (TEM) was carried out with a JEOL 3011 300 kV instrument with a UHR pale piece. The samples for TEM were prepared by dropping the dispersion of MCM-41 in ethanol on a copper grid and drying in ambience. UV−visible diffuse reflectance spectra of powder zeolite samples were collected with an Agilant 8453 spectrophotometer equipped with labsphere RSH-HP-8453 reflectance accessory. Steady state fluorescence measurements of the dye loaded zeolite powder samples were carried out with a Jobin Yuon Fluoromax-4 spectrophotometer at front face configuration at 45°. Time-resolved fluorescence measurements were carried out with (IBH) time correlated single photon counting techniques by exciting the sample at 470 and 635 nm for thionine and methylene blue, respectively. Fluorescence decay was measured at the front face configuration with suitable cutoff filters to avoid scattered light. The data analysis was carried out by the software provided by IBH (DAS-6), which is based on deconvolution techniques using the nonlinear least-squares method, and the quality of the fit is normally identified by the value $\chi^2 < 1.2$ and weighted residual.

Femtosecond emission transient spectra were recorded with the fluorescence up-conversion technique. In the femtosecond up-conversion setup (FOG 100, CDP) the sample was excited with the second harmonic (445 nm) of a mode locked Ti-sapphire laser (Tsunami, Spectra Physics) pumped by DPPS (Millennia, Spectra Physics). The fundamental beam was frequency doubled in nonlinear crystal (1 mm BBO, $\theta = 25°$, $\phi = 90°$). The powder sample was placed in a 1 mm thick rotating cell at front face configuration. The fluorescence emitted from the sample was up-converted in a nonlinear crystal (0.5 mm BBO, $\theta = 38°$, $\phi = 90°$) by using a gate pulse of the fundamental beam. The up-converted light beam is dispersed through a double monochromator and detected by using photon counting technique. The instrument response function of the apparatus was 300 fs. The fluorescence decay was fitted to a Gaussian shape for the excitation pulse. The femtosecond fluorescent decay transients were analyzed by fixing the longer lifetime component obtained from TCSPC. All the experiments were carried out at 293 ± 10 K.

**TABLE 1: The Adsorption Characteristics of Zeolite in the Presence and Absence of the $TiO_2$ Nanoparticles**

| sample | BET surface area, $m^2/g$ | micropore vol, $cm^3/g$ | % $TiO_2$ loading |
|---|---|---|---|
| Zeolite-Y | 645 | 0.265 | 0.00 |
| $TiO_2$-Y (0.08%) | 604 | 0.261 | 0.08 |
| $TiO_2$-Y (1.07%) | 306 | 0.13 | 1.07 |
| ZSM-5 | 453 | 0.167 | 0.00 |
| $TiO_2$-ZSM-5 (0.03%) | 385 | 0.14 | 0.03 |
| $TiO_2$-ZSM-5 (0.08%) | 352 | 0.129 | 0.08 |
| $TiO_2$-ZSM-5 (0.14%) | 260 | 0.098 | 0.14 |

## 3. Results and Discussion

**3.1. Characterization of Titanium Dioxide Loaded Zeolites.** The X-ray diffraction pattern of zeoilite-Y and ZSM-5 in the absence and presence of the titanium dioxide nanoparticals are shown in Figure S1 (Supporting Information). The SAXRD pattern of the titanium dioxide loaded zeolite shows that the crystallinity of the zeolites is unaltered even after the incorporation of titanium dioxide nanoparticles indicating that the structural damage to the host lattice is negligible during the ion-exchange process with the $TiO_2$ particles residing inside the zeolite cavities or channel. However, the crystallinity of the zeolites decreases marginally with increasing titanium dioxide loading above a certain level as reported earlier.[10] The percentage of decrease in crystallinity could be calculated by measuring the intensity of the peak at $2\theta$ values of 8.03° and 6.19° for ZSM-5 and zeolite-Y, respectively. In the case of zeolite-Y a maximum of 5% decrease in crystallinity is observed with the addition of 1.35% by weight titanium dioxide, whereas 12% decrease is observed with the encapsulation of 0.14% titanium dioxide in the channels of ZSM-5. The observed decrease in crystallinity is presumably due to the presence of clusters of $TiO_2$ nanoparticles in the zeolite host. In addition to this, encapsulated titanium dioxide gradually fills the voids of the zeolites, which also contributes to a decrease in the intensity of the peaks in the XRD data.

Adsorption and desorption isotherms of nitrogen on zeolites and $TiO_2$ loaded zeolites are shown in the Supporting Information, Figure S2. Both the zeolites and $TiO_2$ loaded zeolites show clear hysteresis loop. The physicochemical properties of the zeolites in the absence and presence of $TiO_2$ are shown in Table 1. With an increase in the loading of $TiO_2$ into the zeolite-Y, a decrease in the BET surface area is observed with no significant change in XRD pattern revealing that the decrease in the surface area is due to the decrease in the micropore volume of zeolite-Y. The micropore size of zeolite and $TiO_2$ loaded zeolite both have narrow size distribution and narrow average pore width. The pore volume of the zeolite containing maximum loading of the $TiO_2$ is found to decrease from 0.265 $cm^3/g$ to 0.130 $cm^3/g$. The volume of the super cage is calculated to be ~470 $Å^3$, which is an ca. 50% decrease in super cage volume as compared to that of pure Na-zeolite-Y which has the super cage size of 827 $Å^3$. The XRD results and surface area analysis show that titanium dioxide is encapsulated in the cage and channels of the zeolite host (Scheme 1). The transmission electron microscopic (TEM) image (see the Supporting Information, Figure S3) indicates that MCM-41 has ordered mesoporous channels with uniform size while titanium dioxide loaded MCM-41 has less ordered mesoporous channels and is also not able to show titanium dioxide within the channels. These results indicate that the TEM image does not provide detailed information about $TiO_2$ nanoparticles residing inside the channels.

The UV−visible band edge of $TiO_2$ in both zeolites is blue-shifted as compared to that of the bulk anatase (see the Supporting Information, Figure S4). The observed decrease in the band edge in the DRS is due to the size quantization of nanoparticles in the confined geometries. The absorbance value of the sample increases with increase in concentration of titanium dioxide without considerable change in the absorption band edge, which again indicates that the particle size of the $TiO_2$ does not change at higher loading of titanium dioxide in the host material.

**3.2. Influence of $TiO_2$ on the Absorption Spectra of the Dyes in the Silicate Host.** The absorption spectral behavior of thionine and methylene blue in the presence and absence of semiconductor $TiO_2$ nanoparticles inside the channels or cavities of micro- and mesoporous silicate hosts is correlated with the spectral behavior of protonated and unprotonated dye in aqueous solution. The UV−vis absorption spectral behavior of thionine was extensively documented earlier.[14,31−34] The spectrum corresponding to the pure monomeric dye was observed at low concentration ($<1 \times 10^{-5}$ M) of the dye in dilute aqueous solution at about neutral pH. With increasing concentration of the dye, the intensity of the blue-shifted peak shows an enhancement that is known to be due to the formation of the dimer. At pH <0, both the dyes thionine and methylene blue show a red-shift in absorption maximum at 670 and 735 nm respectively. A similar observation was also reported earlier[35] that corresponds to the protonated forms of the dyes at low pH.

Diffuse reflectance spectra of thionine encapsulated into the micro- and mesoporous silicate materials are shown in Figure 1. On the basis of the diffuse reflectance spectra, thionine exists within the channels of ZSM-5 and MCM-41 and is adsorbed onto the external surface of silica as monomeric species. The size of the thionine dye is 11.54 Å × 5.04 Å, which is a planar molecule. However, within the super cage of zeolite-Y, thionine is present predominantly as dimer as indicated by the intense absorption at 550 nm. The formation of the dimeric species of the thionine dye occurs in the free volume available for the guest within the super cage of zeolite-Y. The super cage of zeolite-Y is approximately spherical in nature with a diameter of 13 Å and a free volume of 827 $Å^3$ that is large enough to accommodate H-aggregated thionine molecules. ZSM-5 zeolite consists of two intersecting sets of tubular channels (≈0.54 and 0.56 nm in diameter) defined by a 10-membered ring of $TO_4$ (T = Si or Al) tetrahedra. Thus, three possible adsorption sites in ZSM-5 are straight channels, channel intersection, and sinusoidal channels. Among these three sites of the channels, intersection has large free space for guest molecules having a diameter of 8.7 Å assuming a near-spherical cavity in this space. The cavity does not accommodate H-aggregates since more spherical free volume is needed to include stacked thionine molecules (the stacked dimer can be approximately 15 Å × 7.2 Å × 8 Å). MCM-41 has a tubular channel ~4 nm in diameter and has a larger space to accommodate the dimer. However, no dimer is present as indicated in the absorption spectrum. In this case the polarity of the host with the Si−OH groups plays an important role preventing the formation of dimer. Thionine adsorbed on the silica at the external surface is present only as monomer, since no peak at 550 nm is shown in the absorption spectrum.

Thionine encapsulated into the ZSM-5 channel shows an absorption maximum at 582 nm that is blue-shifted by around 20 nm as compared to the dye in aqueous solution as shown in Table 2. The $\pi-\pi^*$ transitions of the aromatic molecules shift to the red when the molecule is more planar or with increasing aromatic character. Accordingly, in the thionine molecule the lone electron pair on the nitrogen is part of the aromatic system.

**SCHEME 1**

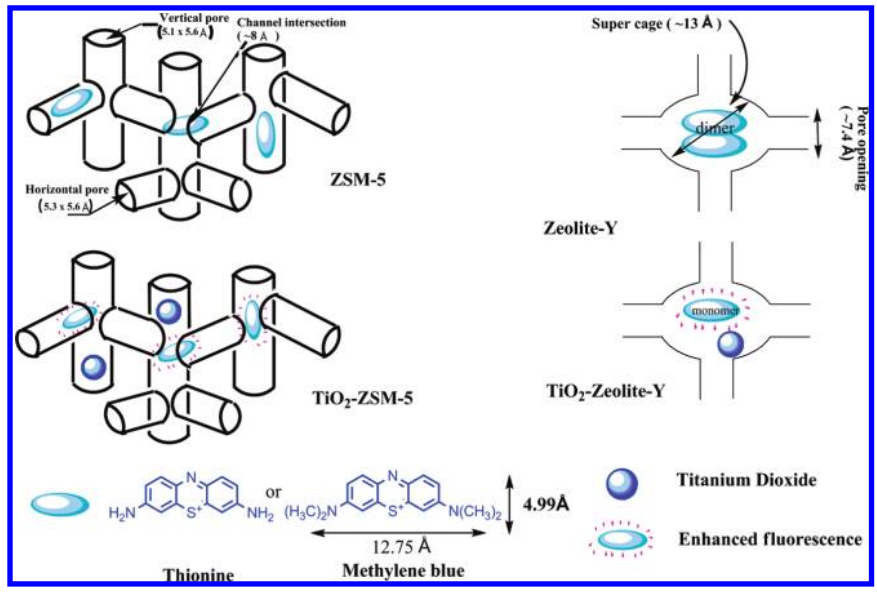


Thionine dye encapsulation in the ZSM-5 channel results in the terminal nitrogen atom tilting out of the aromatic plane due to steric hindrance, causing a blue shift in the absorption spectrum. A similar observation was made in the case of methylene blue present in the interlameller surface, which shows a blue shift in the absorption spectrum due to the change in the orientation of the molecular plane as reported earlier.[36] A similar blue shift is not observed for thionine in the hosts MCM-41, zeolite-Y, and silica due to the presence of larger free space in the host cavity eliminating the possibility of steric hindrance.

The diffuse reflectance spectra of thionine encapsulated into the ZSM-5 and zeolite-Y hosts with different loading levels of titanium dioxide nanoparticles are shown in Figure 2. We observed a new peak at 652 nm for thionine encapsulated into the $TiO_2$ loaded ZSM-5. This observed peak at 652 nm is identified as the protonated form of thionine. The encapsulation of the titanium dioxide leads to an increase in the acidity of the channel of ZSM-5.

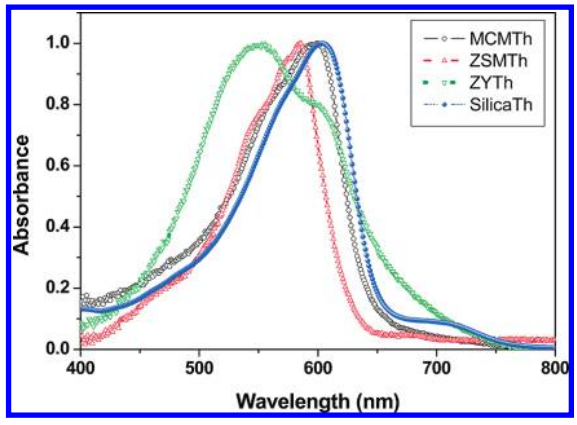


**Figure 1.** Diffuse reflectance spectra of thionine in (●) silica, (○) MCM-41, (△) ZSM-5, and (▼) zeolite-Y.

**TABLE 2: The Photophysical Properties of Thionine Encapsulated into the Micro- and Mesoporous Host Materials[a] ($\chi^2$ Values Are in the Range of 0.99−1.2)**

| sample | $\lambda_{ab}$ max, nm | $\lambda_{emi}$ max, nm | lifetime, ns (% amplitude) |
|---|---|---|---|
| silica-Th | 604 | 626 | 0.27 (88.41%), 2.25 (11.59%) |
| MCM-41-Th | 599 | 626 | 0.16 (2%), 0.31 (98%) |
| ZSM-5-Th | 584 | 612 | 0.33 (66%), 1.77 (44%) |
| zeolite-Y-Th | 550, 602 | | |

[a] The lifetimes reported are within ±0.05 ns.

In the case of zeolite-Y, an increase in the loading of titanium dioxide leads to an enhanced ratio between monomer and dimer because of the reduced free volume available in the void for the formation of H-aggregation of the dye in the zeolite super cage. The dye is loaded onto the host after the encapsulation of $TiO_2$ in the zeolite. The observed results are best correlated with the Brunauer−Emmett−Teller (BET) surface area and powder XRD measurement. Accordingly, zeolite-Y samples containing both thionine and $TiO_2$ nanoparticles are blue in color and showed diffuse reflectance spectra corresponding to the presence of monomeric thionine in the voids. Similar observation has been reported earlier in the case of thionine-doped zeolites in the presence of phenanthrene as the guest molecule.[19] Present observations show that the titanium dioxide is indeed intercalated into the zeolite-Y cavity. Comparing the spectral features of thionine encapsulated into the titanium dioxide loaded ZSM-5 and zeolite-Y, it is concluded that protonation of the dye occurs in the case of ZSM-5. Both zeolite-Y and ZSM-5 are hydrophilic materials and depending up on the framework cations and Si/Al ratio, the charge is known to be different for the atoms present in the lattice.[37] The polarity of the external surface and the surface of the channels and voids depend on the Si/Al ratio, which influences the catalytic activity and conductivity of zeolites.[38] Zeolite-Y is a three-dimensional network with the Si/Al ratio of 2.6 that adsorbs the cationic dye molecule exchanging with the cations ($Na^+$) present in the zeolite framework. The ZSM-5 is a two-dimensional network with the Si/Al ratio of 53.9 leading to an increase in the channel acidity of the material. During the formation of titanium dioxide nanoparticles into the zeolite host the following reaction occurs.[30]

$$TiO^{2+} + H_2O \xrightarrow[\Delta 150^\circ C]{} TiO_2 + 2H^+$$

Accordingly, proton is released to the host materials during the formation of titanium dioxide into the cage or channels of the zeolite that presumably contributes to the protonation

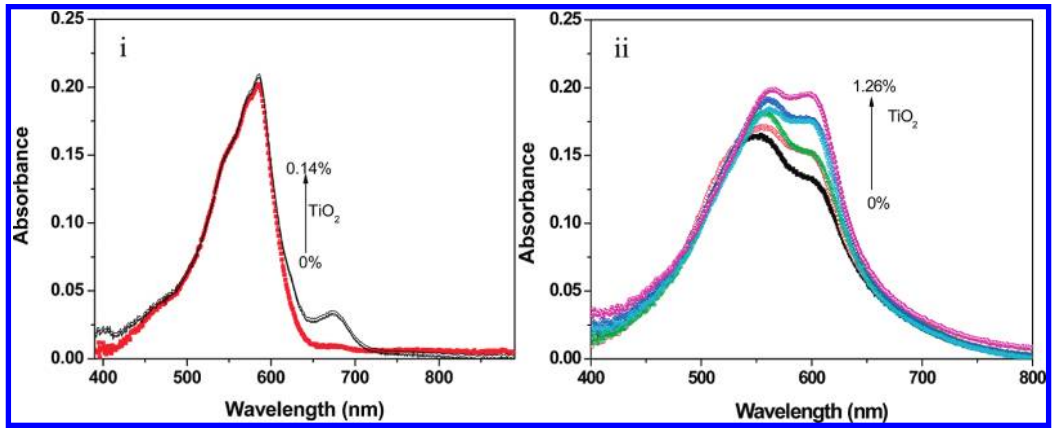


**Figure 2.** Diffuse reflectance spectrum of thionine with different loading levels of $TiO_2$ in (i) ZSM-5 and (ii) zeolite-Y.

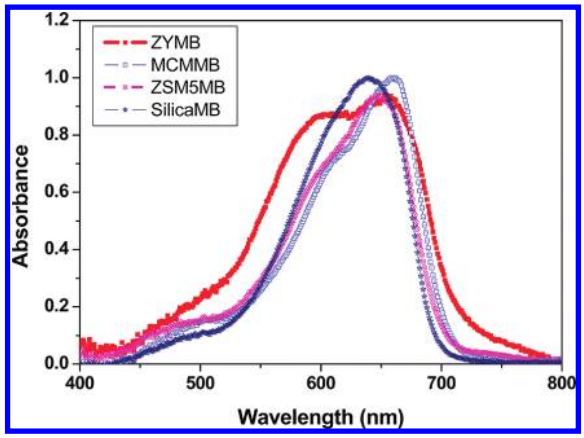


**Figure 3.** Diffuse reflectance spectra of methylene blue in (●) silica, (○) MCM-41, (△) ZSM-5 and (▼) zeolite-Y.

**TABLE 3: The Photophysical Properties of Methylene Blue Encapsulated into the Micro- and Mesoporous Host Materials[a]**

| Sample | $\lambda_{ab}$, nm | $\lambda_{emi}$, nm | lifetime, ns (% amplitude) | av lifetime, ns |
|---|---|---|---|---|
| silica-MB | 640 | 682 | 0.33 (70.99%), 0.78 (29.01%) | 0.46 |
| MCM-41-MB | 660 | 687 | 0.32 (53.58%), 0.69 (46.42%) | 0.49 |
| ZSM-5-MB | 647 | 682 | 0.24 (62.17%), 0.49 (37.83%) | 0.33 |
| zeolite-Y-MB | 600, 658 | 675 | 0.16 (57.72%), 0.52 (42.28%) | 0.31 |

[a] The lifetimes reported are within ±0.05 ns.

of the thionine in the ZSM-5 zeolite. In the case of zeolite-Y, as the nature of the cavity is different due to higher aluminum content, the protonation reaction of the dye does not occur.

The structurally and photophysically very similar but somewhat bulkier molecule methylene blue with two methyl substituents on each of the two amine nitrogen atoms in the same host materials was studied for comparison. Methylene blue encapsulated into channels of ZSM-5 and MCM-41 and adsorbed on silica surface is present as a monomer as indicated in the DRS shown in Figure 3. In the case of $MB^+$ encapsulated in zeolite-Y the absorption spectrum indicates the presence of monomeric and dimeric dye with a lower dimer to monomer ratio in contrast to that observed for thionine in the same host.

The photophysical characteristics of methylene blue adsorbed onto different silicate hosts are given in Table 3. In the case of methylene blue, when adsorbed on silica surface and encapsulated into the ZSM-5 channels, a blue shift in the absorption maximum was observed as compared to that of the dye in aqueous solution. Comparison of the absorption spectra of both dyes, $Th^+$ and $MB^+$, adsorbed on silica surface indicates that the blue shift in the absorption spectrum occurs only in the case of methylene blue. Thionine is a more planar molecule when adsorbed on the surface of silica particles while in the case of $MB^+$ adsorbed on the external surface of silica the methyl groups distort the geometry and hence the observed blue shift. Such a difference can be explained by the nature of hydrogen bonding and planarity of the adsorbed dye molecule on the silica surface. Methylene blue present in the interlameller surface shows a blue shift in the absorption spectrum due to the change in the orientation of the molecular plane as reported earlier.[36] The observed blue shift in absorption is not only due to the change in the planarity of the molecule but also due to hydrogen bonding interaction with the silica surface. The terminal hydrogen on thionine is involved in the hydrogen bonding that results in the red shift in the absorption maximum, whereas in the case of methylene blue the presence of two methyl groups on terminal nitrogen does not lead to the formation of hydrogen bonding with the silica surface. Thus, the blue shift in the absorption spectra of methylene blue adsorbed on the silica surface may be due to the less polar environment provided by the silica surface.

Higher loading of titanium dioxide into the ZSM-5 channels leads to a new absorption peak for the dye at 765 nm corresponding to the protonated form of methylene blue as shown in Figure 4i. The absorbance at 765 nm gradually increases with increase in $TiO_2$ loading when methylene blue is encapsulated in the $TiO_2$ loaded ZSM-5. Similarly, when thionine is encapsulated in the $TiO_2$ loaded ZSM-5, the absorption peak at 656 nm attributed to the protonated form of thionine does not show any significant change with increase in $TiO_2$ loading. Protonation of the dyes in $TiO_2$ loaded ZSM-5 depends on the molecular size and the protonation equilibrium constant of the dye. The protonation equilibrium constants are 0.33 and 4 for thionine and methylene blue, respectively. An increase in the concentration of titanium dioxide into ZSM-5 host leads to enhanced acidity of the host that reaches a maximum and further increase in the concentration of $TiO_2$ does not lead to any additional increase in the absorbance of the protonated form of thionine. In the case of zeolite-Y, with increasing concentration of titanium dioxide, an increase in the absorption at 760 nm is observed that is attributed to the protonated form of methylene blue. Higher loading of titanium dioxide into the zeolite-Y cavities leads to suppression of the aggregation of the dye due to the constriction of the cavity dimension. In the case of $TiO_2$ loaded MCM-41, both the dyes thionine and methylene blue do not show any change in the absorption spectra due to the protonated form of the dye or aggregation of the dye as the channels are larger and the host has no aluminum present. These observations suggest that the

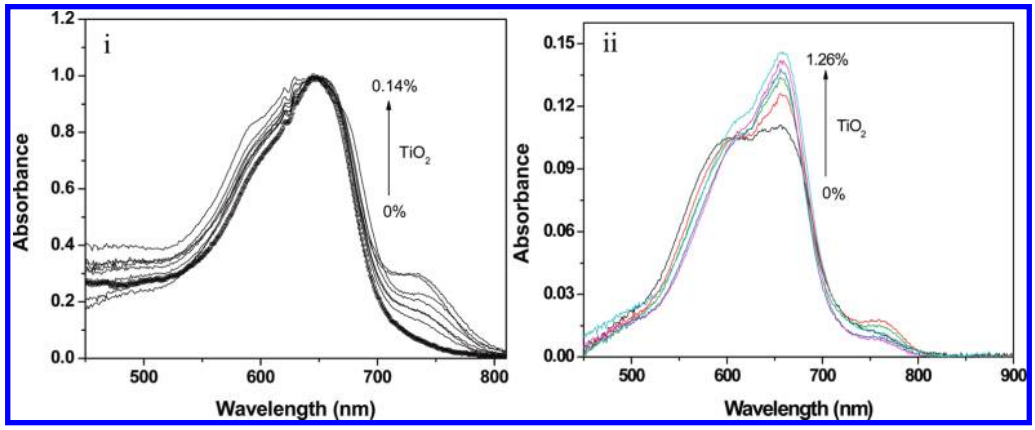


**Figure 4.** Diffuse reflectance spectrum of methylene blue with different loading levels of $TiO_2$ in (i) ZSM-5 and (ii) zeolite-Y.

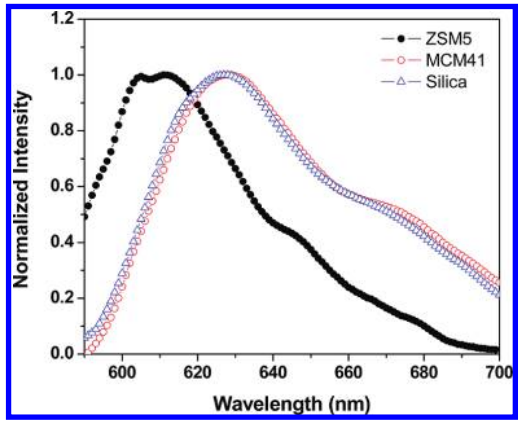


**Figure 5.** Fluorescence emission spectra of thionine with dye concentration given in parentheses in (△) silica ($6.96 \times 10^{-5}$ mol/g), (○) MCM-41 ($6.99 \times 10^{-5}$ mol/g), and (●) ZSM-5 ($7.59 \times 10^{-5}$ mol/g).

protonation of the dyes in the zeolite-Y and ZSM-5 hosts is due to the confinement effect and change in the acidity of the host materials.

**3.3. Fluorescence Spectra and Lifetime of Thionine in the Zeolite Host with Coadsorbed Titanium Dioxide.** ***a. Steady State Emission Behavior of Thionine in the Nanochannels and Nanocavity of the Silicate Hosts.*** Fluorescence emission spectra of thionine adsorbed onto the micro- and mesoporous silicate materials are shown in Figure 5. The emission maximum is observed at 626 nm when the thionine is encapsulated into the MCM-41 channels and adsorbed onto the silica surface. The observed red shift in the emission maximum is due to the interactions of the guest with OH groups of the mesorporous framework and silica surfaces. In these cases, the silica and MCM-41 do not show any confinement effect on the adsorbed thionine molecule. Fluorescence emission was found to be absent for thionine encapsulated into zeolites-Y cavities due to the presence of the aggregated thionine in the cavity. In the case of thionine encapsulated into the channels of ZSM-5, a weak emission is indicated at 612 nm. The observed blue shift in the emission maximum is suggested to be due to the confinement effect of the channel.

The emission spectrum of thionine encapsulated in $TiO_2$ loaded zeolite-Y is shown in Figure 6a. The observed increase in the fluorescence intensity with increasing $TiO_2$ loading is due to the change in the monomer−dimer ratio (note that the dimeric thionine does not show emission). In the case of titanium dioxide loaded MCM-41, such a change in the emission intensity of thionine with increasing loading of $TiO_2$ is not observed (see the Supporting Information, Figure S5). In all three cases the excited state of thionine does not seem to sensitize the titanium dioxide nanoparticles. In an earlier report,[39] it was shown that thionine strongly interacts at the surface of $TiO_2$ colloids in acetonitrile resulting in the quenching of the fluorescence of the dye. Surprisingly, the fluorescence emission intensity of thionine increases with an increase in the loading of titanium dioxide in the ZSM-5 channels and also the emission maximum is red-shifted around 20 nm as compared to that of the thionine in ZSM-5 without $TiO_2$ present. The fluorescence emission spectra of thionine in ZSM-5 loaded with varying concentrations of titanium dioxide are shown in Figure 6b. The 3D contour spectra of thionine in ZSM-5 and $TiO_2$ ZSM-5 are shown in Figure S6 (Supporting Information). A weak emission peak was observed in the absence of $TiO_2$ while in the presence of $TiO_2$ in ZSM-5 a bright emission peak with a maximum at 625 nm is seen. To further elucidate the nature of the excited states and the unusual fluorescence emission behavior, time-resolved emission spectra of the material were carried out in the picosecond and femtosecond time domain.

***b. Time-Resolved Emission Studies of the Dye in Nanochannel and Nanocavity of the Silicate Hosts.*** The fluorescence lifetime of thionine in aqueous solution is known to be 0.34 ns.[40] The fluorescence decay of thionine in these micro- and mesoporous host materials does not fit with single exponential decay and the decay profiles are fitted satisfactorily with biexponential functions. The fluorescence lifetimes of the thionine in the different host materials are given in Table 2. The fluorescence lifetimes of the thionine are lower when the dye is adsorbed on the silica surface as compared to that in water, showing that the dye is strongly adsorbed onto the surface of the host that enhances the nonradiative decay.

Thionine encapsulated into the MCM-41 host shows a lifetime of 0.31 ns (98%), which is very similar to that of the emission behavior of the dye in aqueous solution; in this case dye molecules are presumably present along with water molecules adsorbed in the larger pore of the MCM-41 channel. The fluorescence lifetime of thionine encapsulated into the $TiO_2$ loaded MCM-41 does not change with increasing titanium dioxide loading. In the case of thionine encapsulated into zeolite-Y with 1.25% $TiO_2$, fluorescence lifetimes of 0.15 ± 0.02 ns (71%) and 0.39 ± 0.02 ns (28.93%) are observed. At lower levels of $TiO_2$ loaded zeolite-Y, the emission is very weak and the lifetime could not be determined. The presence of higher aluminum content in the zeolite-Y host and also the dimer formation in the cavity presumably lead to very low emission yield. Thionine encapsulated in ZSM-5 shows a lifetime of 1.7 ± 0.02 ns (44%) and 0.33 ± 0.02 ns (66%); the observed

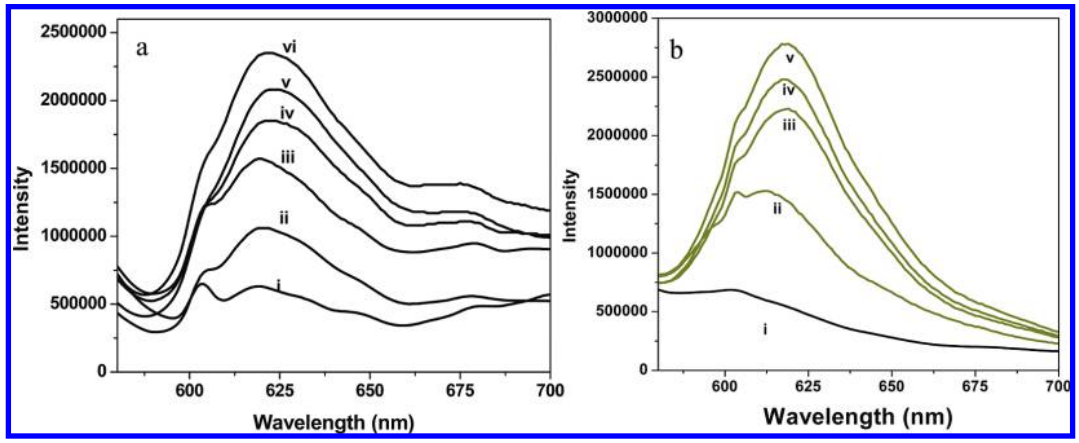


**Figure 6.** Fluorescence emission spectra of thionine with different loading levels of $TiO_2$ in (a) zeolite-Y (i) 0%, (ii) 0.14%, (iii) 0.31%, (iv) 0.74%, (v) 1.07%, and (vi) 1.25% and (b) ZSM-5 zeolite (i) 0% (ii) 0.01%, (iii) 0.025%, (iv) 0.075%, and (v) 0.138%.

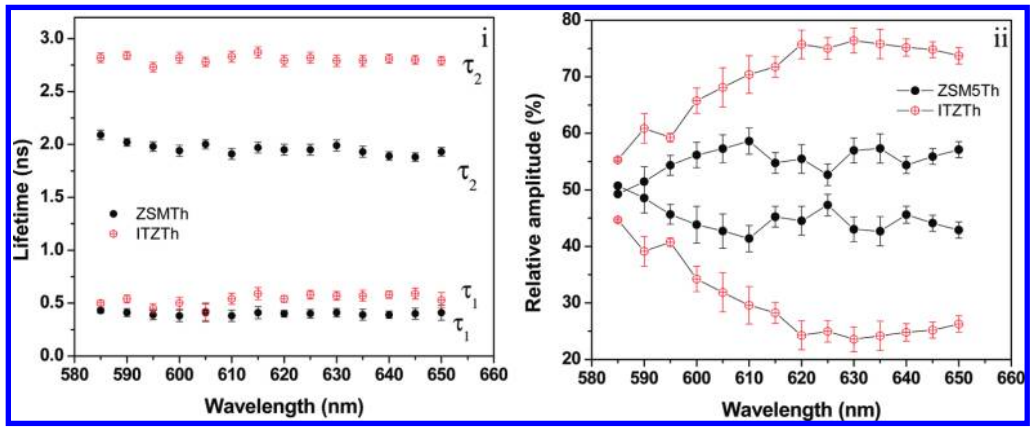


**Figure 7.** Wavelength-dependent fluorescence lifetime (i) and relative amplitude (ii) of thionine encapsulated into ZSM-5 and $TiO_2$/ZSM-5.

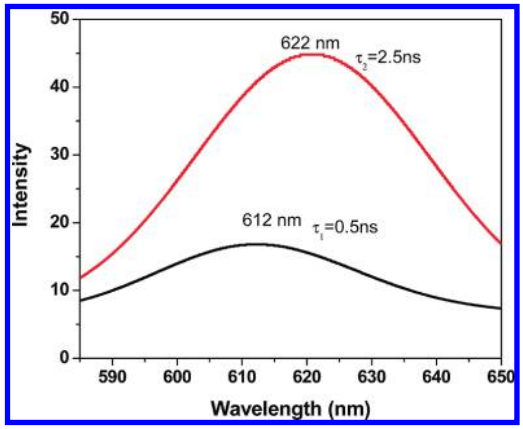


**Figure 8.** The decay associated spectra of thionine in $TiO_2$ loaded ZSM-5.

**SCHEME 2: Two Different Forms of Thionine**

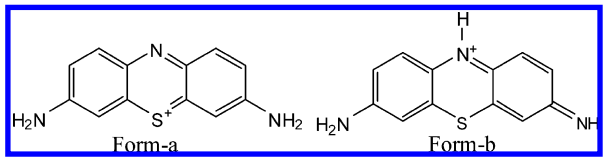


biexponential decay is due to either the dye existing in two different isomeric forms in the excited state or the dye being present at different environments in the host surface. In an earlier report[40] it was shown that thionine covalently attached to a polymer matrix shows biexponential decay. The polymer bound dye molecules which are exposed to the solvent show a lifetime similar to the unbound free dye molecule in aqueous medium and the dye molecules which are located inside the hydrophobic polymer coil show long-lived emission due to a less polar environment for the excited state. These observations suggest that the dye molecule that is present in the channel intersection of the silicate host shows a lifetime 0.33 ns (66%), similar to that in aqueous solution; in this case, the dye molecule is present along with water molecules in the larger pore of the channel intersection. The dye molecules that are present in the vertical channel or sinusoidal channels of ZSM-5 show a longer lifetime of 1.7 ns (44%) in the hydrophobic environment of the excited state. To further elucidate the nature of excited state processes of thionine in $TiO_2$ loaded ZSM-5, we have carried out the picosecond and femtosecond time-resolved fluorescence spectral studies (vide infra).

The fluorescence decay of thionine within the nanochannel of ZSM-5 is observed to be biexponential throughout the emission wavelength from 585 to 650 nm. The observed fluorescence lifetimes and relative amplitudes at different emission wavelength are identical and are shown as a function of wavelength in Figure 7. In the case of titanium dioxide loaded ZSM-5, the dye molecule shows an increase in the fluorescence lifetime as compared to that of dye in ZSM-5. However, the observed lifetimes are identical in the entire emission wavelength and the relative amplitudes vary with emission wavelength as shown in Figure 7ii. This observation indicates that the thionine dye exists in two different forms in the excited state.

The two discrete excited states corresponding to the lifetime components observed in the host material could not be resolved in the steady state emission spectra. The distinct lifetime profiles of the dye encapsulated in ZSM-5 hosts readily allow the

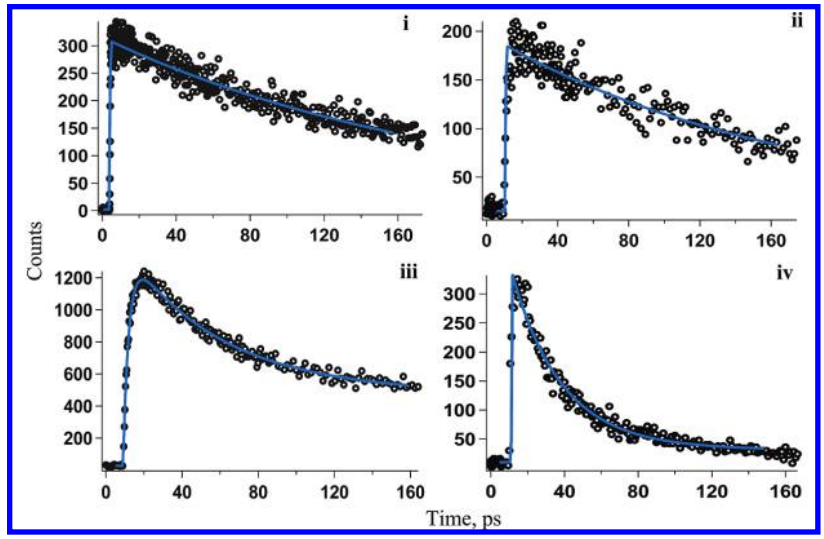


**Figure 9.** Femtosecond florescence decay of thionine in (i) aqueous solution at 620 nm, (ii) MCM-41 at 630 nm, (iii) ZSM-5 at 630 nm, and (iv) ZSM-5 at 585 nm.

resolution of the emission behavior using time-resolved methods. The excitation wavelength used for the dye in ZSM-5 host is 470 nm and the decay was recorded every 5 nm across the emission wavelength from 585 to 650 nm.

We have constructed decay-associated spectra from the fluorescence decay data at different emission wavelengths, which distinguishes the presence of the different species in the excitation spectra. Decay associated spectra of thionine in $TiO_2$ loaded ZSM-5 are shown in Figure 8. Interestingly, quite different emission spectra were obtained for the two lifetimes with maximum at 612 (0.5 ns) and 625 nm (2.5 ns) for thionine in titanium dioxide loaded ZSM-5. The decay-associated spectrum with 2.5 ns component shows maximum intensity distribution as compared to that of the short lifetime component that indicates that two different forms of thionine are present in $TiO_2$ loaded ZSM-5 host and the contribution of the two forms varied with channel acidity.

Such an observation suggesting two forms of thionine in the excited state was reported earlier.[33,41] Deeg[33] et al. suggest that thionine exists in two forms in the dehydrated zeolite-Y voids, which can be separately observed and which convert into each other showing different fluorescence quantum yields for the two forms. Weng[41] et al. also identified that thionine exists in two forms a-form and b-form in glycerol−water glass. These tautomers are matrix-dependent and the acidic protons present in the host matrix are responsible for the appearance of the two tautomers; the two tautomers are depicted in Scheme 2.

On the basis of the above observations, the interpretation is that thionine present in the channels of ZSM-5 exists in two forms in the excited state exhibiting different quantum yields and the two forms are interconvertible. The dye present in the hydrophilic environment of the ZSM-5 host causes a blue shift in the absorption spectra with a decrease in emission intensity. The hydrophobicity of the host increases with increase in the loading of titanium dioxide in the ZSM-5 host. The dye present in the hydrophobic environment leads to an increase in the fluorescence quantum yield that enhances the emission intensity with the emission spectral maximum red-shifted. The zeolite acidity and confinement effect of the channels play a crucial role in the separation of the two forms of thionine in the excited state. This conclusion is best correlated with the steady state emission spectra of thionine encapsulated into the ZSM-5 and $TiO_2$ loaded ZSM-5.

**TABLE 4: Time Constants ($\tau$) and Normalized Pre-exponential Factors ($a$) of Functions Used in Fitting the Femtosecond Emission Transients of Thionine in Various Host Materials and in Aqueous Solution**

| Sample | $\tau_1$ /ps | $a_1$/% | $\tau_2$ /ps | $a_2$/% | $\tau_3$[a] /ps | $a_3$/% |
|---|---|---|---|---|---|---|
| Th-aqueous | | | | | 268 | 100 |
| Th-MCM-41 | | | | | 160 | 100 |
| Th-ZSM-5 | | | 30[b] | 42.36 | 595 | 57.63 |
| | 2.6 | –3.11 | 46[c] | 48.81 | 530 | 54.30 |
| Th-$TiO_2$/ZSM-5 | | | 24[b] | 30.13 | 936 | 69.86 |
| | 3 | –0.58 | 47[c] | 6.31 | 1110 | 94.27 |

[a] Average lifetime obtained from TCSPC. [b] Decay monitored at 585 nm. [c] Decay monitored at 630 nm.

**3.4. Femtosecond Dynamics of Thionine within the ZSM-5 Channels.** To probe the excited state interconversion between two forms of thionine in nanochannels of ZSM-5, femtosecond up-conversion experiments were performed. The representative femtosecond fluorescence decay of thionine in aqueous solution and in different host materials is shown in Figure 9. The data (time and relative amplitude) obtained from the femtosecond decay is given in Table 4. The dye encapsulated into the MCM-41 and in aqueous solution shows a single exponential decay of fluorescence. The observed femtosecond decay profiles for the emission with femtosecond experiments are in good agreement with those obtained from the picosecond data. When the femtosecond emission decay was monitored at 585 nm (the blue side of the emission spectra), the decay curve consisted of a rapidly decaying ($\tau = 23$ ps) component and a slower one (595 ps). The emission monitored at 630 nm (the red side of the emission spectrum) exhibits rising intensity with $\tau = 2$ ps (the pre-exponential factor of this term was negative) followed by long-lived decay components (45 and 595 ps). The observed short lifetime component suggests a multiexponential decay of emission due to interconversion of two excited state species. At shorter time scale (0−1 ns), the emission spectrum has a peak at 612 nm and at longer time (3 ns) the peak appears at 625 nm. This observation demonstrates that some initially formed excited state species A* is converted into a second form B* and the emission spectrum B* is red-shifted relative to A* by around 15 nm. As discussed in the previous section, in ZSM-5, thionine is present in two different environments, i.e., channels and channel intersection. The dye present in channel intersection does not undergo excited state interconversion whereas thionine present in straight and sinusoidal channel undergoes excited state

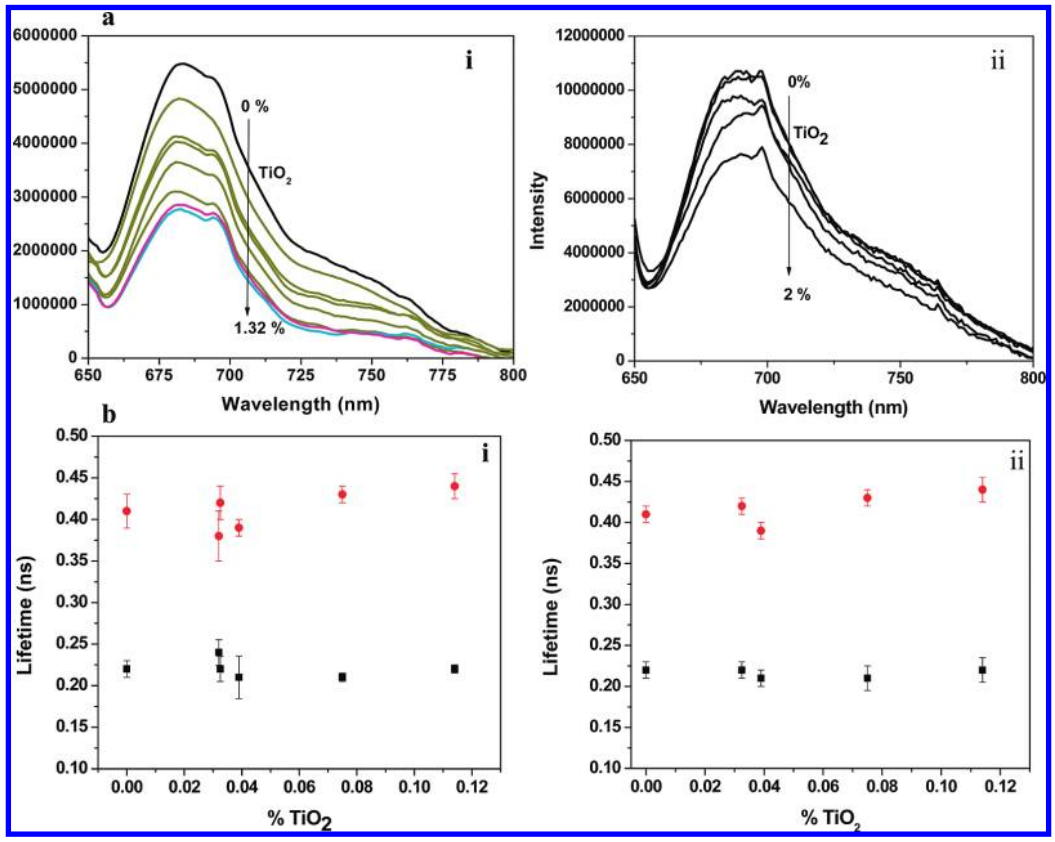


**Figure 10.** (a) Fluorescence emission spectra of methylene blue with different loading levels of $TiO_2$ (i) ZSM-5 and (ii) MCM-41, and (b) fluorescence lifetime of methylene blue in (i) ZSM-5 and (ii) MCM-41 containing various loading level of titanium dioxide.

interconversion due to the hydrophobicity present in the channels. The observed 23 and 45 ps lifetimes are presumably due to the excited state relaxation of thionine in nanochannels of ZSM-5. The relaxed state emission of thionine could not be observed due to close spectral overlap of A and B forms of thionine. The above observations indicate that such a multistate emission behavior is not observed in the case of thionine encapsulated in MCM-41. The present investigation with the thionine encapsulated in ZSM-5 shows that synthesized guest−host combinations with the appropriate choice of chromophores and nanostructured cavity could lead to novel devices with control on the degrees of freedom, photophysics, and mobility of the guest molecule.

**3.5. Influence of $TiO_2$ on the Fluorescence Spectra and Lifetime of Methylene Blue in Zeolite Host.** The fluorescence emission maxima of methylene blue in micro- and mesoporous silicate hosts are given in Table 3. Methylene blue encapsulated in MCM-41 and ZSM-5 and adsorbed on the silica surface shows a red-shift in the fluorescence emission maximum as compared to that of the dye in aqueous solution indicating the interaction of the excited state of methylene blue with the silicate host. Methylene blue encapsulated into the zeolite-Y shows a week emission at 675 nm that is similar to that of the dye in aqueous solution. The observed spectral behavior of the dye similar to that in aqueous solution is interpreted to be due to the presence of larger free space available in the zeolite-Y cavity. In this case, the dye molecule is present along with the water molecules in the larger super cage of zeolite-Y.

The fluorescence lifetime of methylene blue in water is found to be 0.4 ns as reported earlier.[42] The fluorescence decay curves of methylene blue in silicate hosts fit bi exponential function satisfactorily. The observed biexponential is suggested to be due to the heterogeneity of the site for the dye in the silicate host. The average fluorescence lifetime of the dye adsorbed in silica surface and encapsulated in MCM-41 channel is similar to that obtained in aqueous solution. In the case of $MB^+$ encapsulated into the ZSM-5 and zeolite-Y a decrease in the average fluorescence lifetime is observed that is due to the presence of the aluminum in the zeolite framework.

Methylene blue coadsorbed with titanium dioxide in the nanochannels of ZSM-5 shows a decrease in the fluorescence intensity as shown in Figure 10ai. The observed fluorescence quenching is suggested to be due to electron transfer from the excited state of $MB^+$ to encapsulated titanium dioxide in ZSM-5; we have earlier reported such quenching processes for the dyes in silicate hosts.[10,11] The fluorescence lifetime of methylene blue is found to be unaltered significantly with the increase in the loading of titanium dioxide as indicated in Figure 10bi, even though a decrease in fluorescence intensity has been observed in the steady state experiments. These results indicate that the observed decrease in the fluorescence intensity is due to electron transfer from the dye in the excited state to the semiconductor nanoparticles and the quenching process is static in nature; the excited dye and the semiconductor are in contact in the host surface. Methylene blue encapsulated into the $TiO_2$ loaded zeolite-Y shows an increase in the emission intensity due to change in the monomer−dimer ratio of the dye. The average fluorescence lifetime of the methylene blue coadsorbed with titanium dioxide in zeolite-Y shows an increase from 0.31 to 0.40 ns and is found to be similar to that of the dye in aqueous solution, which indicates that an increase in the loading of the titanium dioxide leads to a decrease in the free volume available for accommodation of dimer in the super cage. In this case, dye molecules are present along with the water molecules in the super cage of zeolite-Y. Methylene blue encapsulated into the $TiO_2$ loaded MCM-41 shows a decrease in the fluorescence

emission intensity (Figure 10bii) suggesting charge transfer from the excited state of methylene blue to the semiconductor nanoparticle. The fluorescence lifetime of methylene blue encapsulated into the $TiO_2$ loaded MCM-41 does not change with increasing titanium dioxide loading as shown in Figure 10bii, illustrating that the quenching process is static in nature. The present investigation with $MB^+$ in porous silicate host shows photosensitization of the titanium dioxide nanoparticles in the silicate host by coadsorbed dye molecules.

## 4. Conclusion

Thionine and methylene blue dyes are incorporated in nanoporous silicate hosts, MCM-41, ZSM-5, zeolite-Y, and silica. The results of XRD and surface area measurement support the fact that the $TiO_2$ is located inside the zeolite matrix. It was observed that the protonation and aggregation of the dyes depend strongly on the size and acidity of the nanochannels and nanocavities of silicate hosts. Controlled aggregation of thionine in zeolite-Y is observed. Thionine in $TiO_2$ loaded ZSM-5 undergoes excited state interconversion into isomers that is confirmed by picosecond and femtosecond fluorescence studies. In the case of thionine encapsulated in $TiO_2$ loaded ZSM-5 host shows two species of the excited states of the dye. In the femtosecond up-conversion technique it has been observed that the initially excited thionine relaxes to a lower excited state in about 2 ps. These two excited state species of the dye show emission with maxima at 612 and 625 nm. The thionine dye encapsulated in MCM-41 host does not show this behavior. Methylene blue encapsulated in MCM-41 and ZSM-5 loaded with $TiO_2$ shows the charge transfer process from the excited state of the dye to the semiconductor as revealed by the steady state and time-resolved emission spectral studies.

**Acknowledgment.** The authors acknowledge the financial support received from the Department of Science and Technology, Government of India through the Raja Ramanna Fellowship to one of the authors (P.N.). The center is supported by the DST-IHRPA program. The XRD and surface area measurements were carried out at CSMCRI, Bhavnagar with the permission of the Director, CSMCRI.

**Supporting Information Available:** X-ray diffraction pattern of zeoilite-Y and ZSM-5 in the absence and presence of the titanium dioxide nanoparticals, adsorption and desorption isotherms of nitrogen on zeolites and $TiO_2$ loaded zeolites, TEM image of MCM-41, diffuse reflectance spectra of $TiO_2$ nanoparticles into the ZSM-5 zeolite and zeolite-Y, and contour spectra of thionine encapsulated into the ZSM-5 and $TiO_2$ loaded ZSM-5. This material is available free of charge via the Internet at http://pubs.acs.org.

## References and Notes

(1) Kamat, P. V. *J. Phys. Chem. C* **2007**, *111*, 2834–2860.
(2) Tvrdy, K.; Kamat, P. V. *J. Phys. Chem. A* **2009**, *113*, 3765–3772.
(3) Gil, M.; Wang, S.; Organero, J. A.; Teruel, L.; Garcia, H. Douhal. *J. Phys. Chem. C* **2009**, *113*, 11614–11622.
(4) Bruhwiler, D.; Gfeller, N.; Calzaferri, G. *J. Phys. Chem. B* **1998**, *102*, 2923–2929.
(5) Bussemer, B.; Munsel, D.; Wunscher, H.; Mohr, G. J.; Grummt, U. *J. Phys. Chem. B* **2007**, *111*, 8–15.
(6) Fujii, K.; Iyi, N.; Hashizume, H. *Chem. Mater.* **2009**, *21*, 1179–1181.
(7) Harris, C.; Kamat, P. V. *ACS Nano* **2009**, *3*, 682–690.
(8) Yui, T.; Tsuchino, T.; Itoh, T.; Ogawa, M.; Fukushima, Y.; Takagi, K. *Langmuir* **2005**, *21*, 2644–2646.
(9) Fujii, K.; Iyi, N.; Sasai, R.; Hayashi, S. *Chem. Mater.* **2008**, *20*, 2994–3002.
(10) Eswaramoorthi, S.; Natarajan, P. *Microporous Mesoporous Mater.* **2009**, *117*, 541–550.
(11) Ananthanarayanan, K.; Natarajan, P. *Microporous Mesoporous Mater.* **2009**, *124*, 179–189.
(12) Shim, T.; Lee, M. H.; Kim, D.; Yoon, K. B. *J. Phys. Chem. B* **2009**, *113*, 966–969.
(13) Eswaramoorthi, S.; Natarajan, P. *J. Porous Mater.* **2008**, *15*, 343–349.
(14) Kongkanand, A.; Kamat, P. V. *ACS Nano* **2007**, *1*, 13–21.
(15) Kemnitz, K.; Yoshihara, K.; Ohzaki, K. *J. Phys. Chem.* **1990**, *94*, 3099–3104.
(16) Spitler, M. T. *J. Imaging Sci.* **1991**, *35*, 351–355.
(17) Law, K. Y. *Chem. Rev.* **1993**, *93*, 449–486.
(18) Das, S.; Kamat, P. V. *J. Phys. Chem. B* **1999**, *103*, 209–215.
(19) Ramamurthy, V.; Sandeson, D. R.; Eaton, D. F. *J. Am. Chem. Soc.* **1993**, *115*, 10438–10439.
(20) Fujishima, A.; Rao, T. N.; Tryk, D. A. *J. Photochem. Photobiol., C* **2000**, *29*, 1–21.
(21) Gratzel, M.; Regan, B. O. *Nature* **1991**, *353*, 737–740.
(22) Chen, X.; Mao, S. S. *Chem. Rev.* **2007**, *107*, 2891–2959.
(23) Panpa, W.; Sujardworakam, P.; Jinawath, S. *Appl. Catal., B* **2008**, *80*, 271–276.
(24) Klimenkov, M.; Nepijko, S. A.; Watz, M. *J. Cryst. Growth* **2001**, *231*, 577–588.
(25) Juite, E.; Kely, J. M. *J. Photochem. Photobiol., B* **1993**, *21*, 103–124.
(26) Hagmar, P.; Pierrou, S.; Nielson, P.; Norden, B.; Kubista, M. *J. Biomol. Struct. Dyn.* **1992**, *9*, 667.
(27) Segar, B.; Vinodgopal, K.; Kamat, P. V. *Langmuir* **2007**, *23*, 5471–5476.
(28) Beck, J. S.; Vartuli, J. C.; Roth, W. J.; Lenowiez, M. E. *J. Am. Chem. Soc.* **1992**, *114*, 10834–10843.
(29) Heger, D.; Jirkovsky, J.; Klan, P. *J. Phys. Chem. A* **2005**, *109*, 6702–6709.
(30) Corrent, S.; Cosa, G.; Scaiano, J. C.; Maria, S. G.; Alvaro, M.; Garcia, H. *Chem. Mater.* **2001**, *13*, 715–722.
(31) Jacobs, K. Y.; Schoonheydt, R. A. *Langmuir* **2001**, *17*, 5150–5155.
(32) Li, F.; Zare, R. N. *J. Phys. Chem. B* **2005**, *109*, 3330–3333.
(33) Ehri, M.; Kindervater, H. W.; Deeg, F. W.; Brauchle, C. *J. Phys. Chem.* **1994**, *98*, 11756–11763.
(34) Liu, S.; Chen, A. *Langmuir* **2005**, *21*, 8409–8413.
(35) Calzaferri, G.; Gfeller, N. *J. Phys. Chem.* **1992**, *96*, 3428–3435.
(36) Cenens, J.; Schoonheydt, R. A. *Clays Clay Miner.* **1998**, *36*, 214–224.
(37) Corma, A. *J. Catal.* **2003**, *216*, 298–312.
(38) Alvaro, M.; Cabeza, J. F.; Fabuel, D.; Garcia, H. *Chem. Mater.* **2006**, *18*, 26–33.
(39) Patrick, B.; Kamat, P. V. *J. Phys. Chem.* **1992**, *96*, 1423–1428.
(40) Viswanathan, K.; Natarajan, P. *J. Photochem. Photobiol., A* **1996**, *95*, 245–253.
(41) Weng, K. C.; Chiang, C. C.; Cheng, J. Y.; Cheng, S. Y.; Cheng, T. C. *Chem. Phys. Lett.* **1999**, *302*, 347–353.
(42) Enescu, M.; Lindqvist, L. *J. Phys. Chem.* **1995**, *99*, 8405–8411.

JP912267Q